BBA 75925

PROPERTIES OF ATPase OF GASTRIC MUCOSA

III. DISTRIBUTION OF HCO_3^--STIMULATED ATPase IN GASTRIC MUCOSA

G. SACHS*, G. SHAH, A. STRYCH, G. CLINE AND B. I. HIRSCHOWITZ

Division of Gastroenterology and Department of Biology, University of Alabama in Birmingham, Birmingham, Ala. (U.S.A.)

(Received November 19th, 1971)

SUMMARY

To further localize the HCO_3^--stimulated SCN^--inhibited ATPase of gastric mucosa, the distribution of several enzymes (HCO_3^--, Mg^{2+}- and ($Na^+ + K^+$)-ATPase, lactate dehydrogenase, NADH oxidase, alkaline phosphatase, inosine diphosphatase and adenosine monophosphatase) was studied in density gradient distribution of the mitochondrial, light mitochondrial and microsomal fractions of the homogenate. It was shown that the HCO_3^--ATPase had markedly different characteristics from the other enzymes, and a hypothesis is presented for the function of this enzyme in gastric secretion.

INTRODUCTION

Although proton transport by the gastric mucosa has been the subject of much theory and much experimentation, the details of the mechanism remain quite obscure. Clearly, however, the specialized structure on the secretory surface of the oxyntic cell (a microtubular system in the case of amphibia, and intracellular canaliculi with similar surface infoldings in the mammalian cell) must play a critical role in the process.

Since the discovery in 1965 by Kasbekar and Durbin[1] of a HCO_3^--stimulated, SCN^--inhibited ATPase (SCN^- being an inhibitor of acid secretion) the possibility of this ATPase being involved in acid secretion has been investigated by several groups of workers. In the same year Sachs *et al.*[2] showed that, although in the gastric mucosa this enzyme was localized in the microsomal fraction as would be expected from an enzyme present in the oxyntic cell vesicles, it was also present in other tissues, and in the case of rat liver, apparently in the mitochondrial fraction. Forte and his group confirmed the presence of this enzyme in a highly purified microsomal fraction[3] from gastric mucosa and further showed that the appearance of this enzyme coincided ontogenetically with the onset of acid secretion in the frog[4].

Parenthetically, Racker[5] had shown that mitochondrial ATPase was also HCO_3^- stimulated, and Sachs and co-workers[6,7] had demonstrated that SCN^- was

Abbreviation: HEPES, *N*-2-hydroxyethylpiperazine-*N'*-2-ethanesulfonic acid.

* To whom correspondence should be addressed.

able to block ATP or ADP binding to the mitochondrial membrane, as well as altering K^+ flux characteristics in mitochondria and intact mucosa.

More recently, it has been shown that the HCO_3^--ATPase of the adult *Necturus* gastric mucosa is localized exclusively in the oxyntic cells[8] and moreover that a considerable fraction of this enzyme is present in smooth surfaced vesicles presumably derived from the tubular system of that cell.

The enzyme has been similarly localized in other species[9] and is also present in high concentration in the pancreas (B. Simon, R. Kinne and G. Sachs, to be published). However, in that organ the highest specific activity is found in the $1 \cdot 10^5 \times g \cdot$min fraction but density gradient fractionation localizes it in a particle of identical density to the gastric mucosal vesicle. Since, therefore, it is important to decide whether the gastric enzyme is derived from mitochondria, or whether a similar enzyme is also present in gastric mitochondria, a series of experiments was undertaken to determine the activity of several different enzymes in various fractions from continuous gradient distribution of the $1 \cdot 10^5 \times g \cdot$min, $4 \cdot 10^5 \times g \cdot$min, $6 \cdot 10^6 \times g \cdot$min pellets.

METHODS

Fresh dog gastric mucosa was scraped off the underlying connective tissue, homogenized in 0.25 M sucrose buffered with 20 mM *N*-2-hydroxyethylpiperazine-*N'*-2-ethanesulfonic acid (HEPES) at pH 7.4, using a teflon glass homogenizer. The dilution was 1:20 to reduce mucus interference with the fractionation. The homogenate was spun at 1000 $\times$ *g* for 10 min, the precipitate washed once and the combined supernatants spun at 5000 $\times$ *g* for 20 min. The pellet was again washed and the supernatant spun at 20000 $\times$ *g* for 20 min, the pellet at this stage washed again and the 100000 *g*·60 min pellet obtained from the supernatant. At this stage the $4 \cdot 10^5$ and $6 \cdot 10^6 \times g \cdot$min pellets were suspended in 0.25 M sucrose and layered on a linear 18–47.5 % buffered sucrose gradient 20 mM HEPES (pH 7.4) and centrifuged for 16 h at 23500 rev./min in a Spinco SW25 rotor whereas the $10^5 \times g \cdot$min was layered on a 25–63 % linear gradient. Successive 1-ml fractions were obtained from the tubes for analysis. Sucrose concentration was measured with an Abbé refractometer, and protein measured spectrophotometrically at 280 nm. ATPase, Mg^{2+} dependent, $Na^+ + K^+$ stimulated and HCO_3^- stimulated and CNO^- inhibited, was measured as previously described[9]. NADH oxidase was measured by the reduction of dichlorophenol indophenol[10], succinate dehydrogenase by the method of King[11], acid and alkaline phosphatase by *p*-nitrophenyl phosphate hydrolysis at pH 2.8 and pH 10.5, respectively. Inosine diphosphatase and 5'-nucleotidase were measured by measuring the phosphate released by the method of Yoda and Hokin[12] from inosine diphosphate and adenosine monophosphate. Monamine oxidase was measured by following the formation of benzaldehyde at 250 nm from benzylamine in a Gilford recording spectrophotometer according to the method of Tabor *et al.*[13] and lactate dehydrogenase as described by Reeves and Fimognari[14]. The HCO_3^--ATPase was solubilized using Triton X-100 as described in an earlier paper of this series and the effect of other anions on enzyme activity measured as before[9].

Total enzyme activities were expressed as follows per ml of gradient: (a) ATPase, IDPase as μmoles P_i released per h; (b) acid phosphatase as $\Delta A_{400\,nm} \cdot 2.76$ per h $\equiv$

units; (c) alkaline phosphatase as $\Delta A_{400\ nm} \cdot 11.82$ per h $\equiv$ units; (d) succinate dehydrogenase as μmoles succinate oxidized per min $\equiv$ units; (e) NADH dehydrogenase as μmoles NADH oxidized per min $\equiv$ units;(f) monamine oxidase as $\Delta A_{250\ nm}$ per min $\equiv$ units.

Specific activities were expressed as μmoles or units per mg protein per unit time (h or min as required). Electron microscopy was performed on 1 % OsO_4-fixed pellets embedded in Epon. 1-μm sections were examined in a Phillips EM 200 electron microscope at 60 kV.

RESULTS

Protein distribution

The experiments described were reproducible in 3 separate runs.

The $1 \cdot 10^5 \times g \cdot$min fraction when banded on a linear gradient of buffered sucrose showed a trace band at the entry point of the gradient, and a single obviously heterogeneous band with a peak at 40.5 % sucrose (Fig. 1). Electron microscopy of the $1 \cdot 10^5 \times g \cdot$min starting material showed considerable heterogeneity, comprising (a) mitochondria; (b) tubular complex fragments; (c) zymogen granules; (d) glycogen granules and (e) mucus granules. The band obtained from the gradient contained mostly mitochondria and large membrane fragments.

The $4 \cdot 10^5 \times g \cdot$min fraction showed a major protein peak at 41.5 % sucrose with minor peaks at 31 and 37 % sucrose (Fig. 2). Electron microscopy of the $4 \cdot 10^5 \times g \cdot$min fraction showed it to contain (a) small mitochondria and mitochondrial fragments, (b) again membrane or "tubular complex" fragments smaller than in the previous fraction, and (c) "rough" endoplasmic reticulum. The major protein band on the gradient, however, contained mostly small mitochondria.

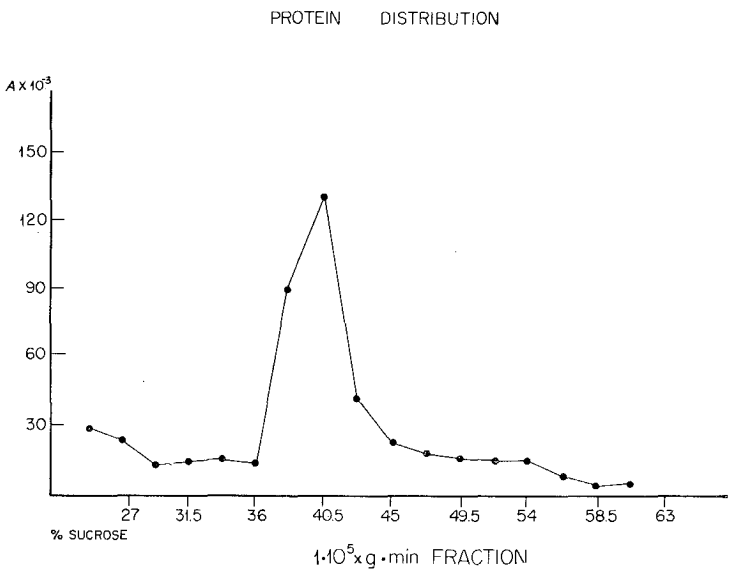

Fig. 1. Protein distribution of $1 \cdot 10^5 \times g \cdot$min fraction run in a linear sucrose gradient (25–63 %, w/w) at 5 °C, in a Spinco SW25 rotor for 16 h at 22000 rev./min.

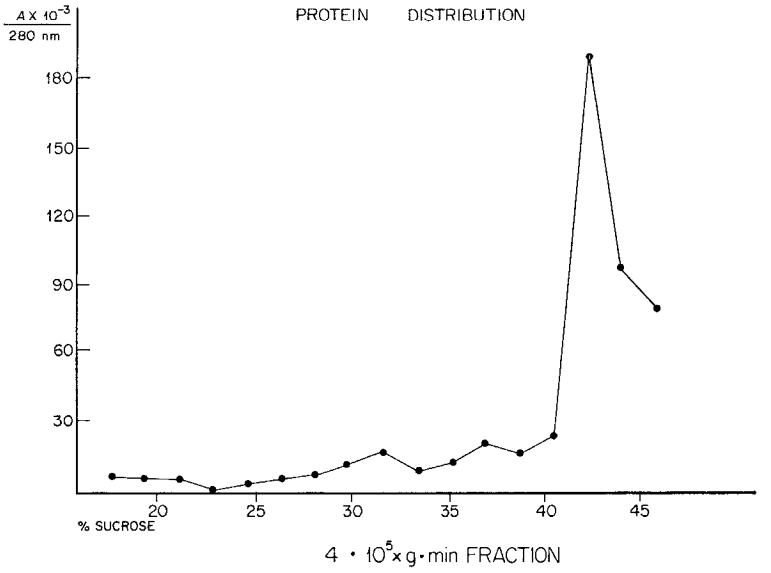

Fig. 2. Protein distribution of the $4 \cdot 10^5 \times g \cdot$min fraction run in a linear sucrose gradient (18–47.5%, w/w) under the same conditions as in Fig. 1.

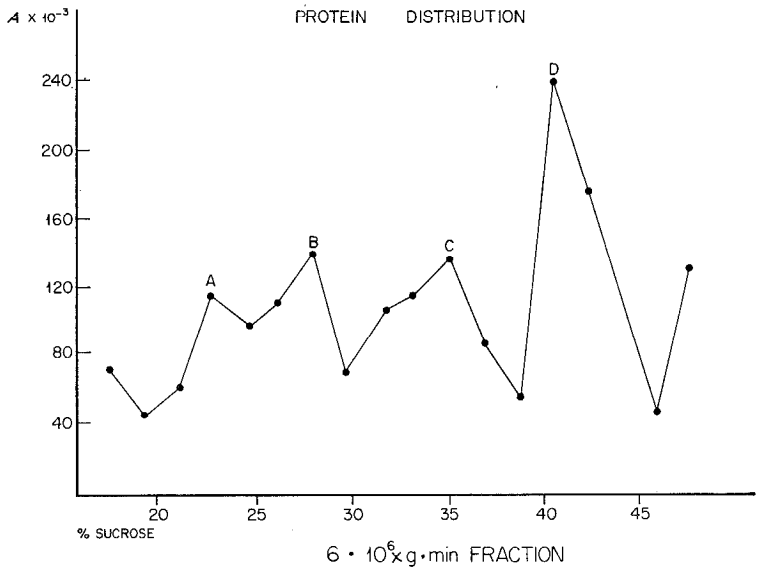

Fig. 3. Protein distribution of the $6 \cdot 10^6 \times g \cdot$min fraction run under the same conditions as in Fig. 2.

The $6 \cdot 10^6 \times g \cdot$min fraction banded on the sucrose gradient giving 4 protein peaks, as in Fig. 3. The first 2 bands were not structurally distinguishable in the

electron microscope, consisting almost entirely of smooth surfaced vesicles as shown in ref. 9. The last 2 bands consisted mostly of what appeared to be mitochondrial fragments, and of a mixture of membrane-like material and various types of granules.

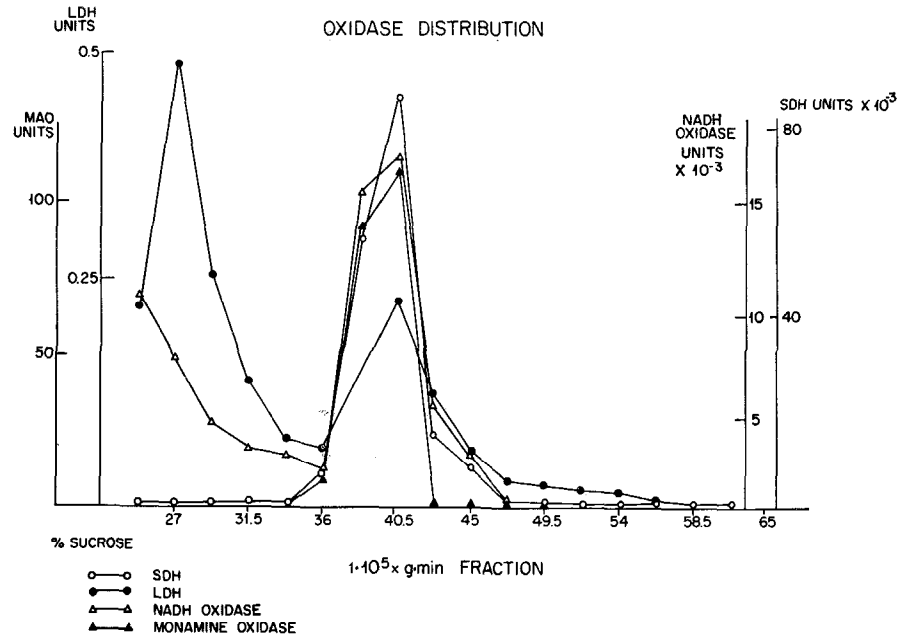

Fig. 4. Distribution of monoamine oxidase (MAO), NADH oxidase, lactate dehydrogenase (LDH) and succinate dehydrogenase (SDH) in the gradient from the $1 \cdot 10^5 \times g \cdot$min precipitate.

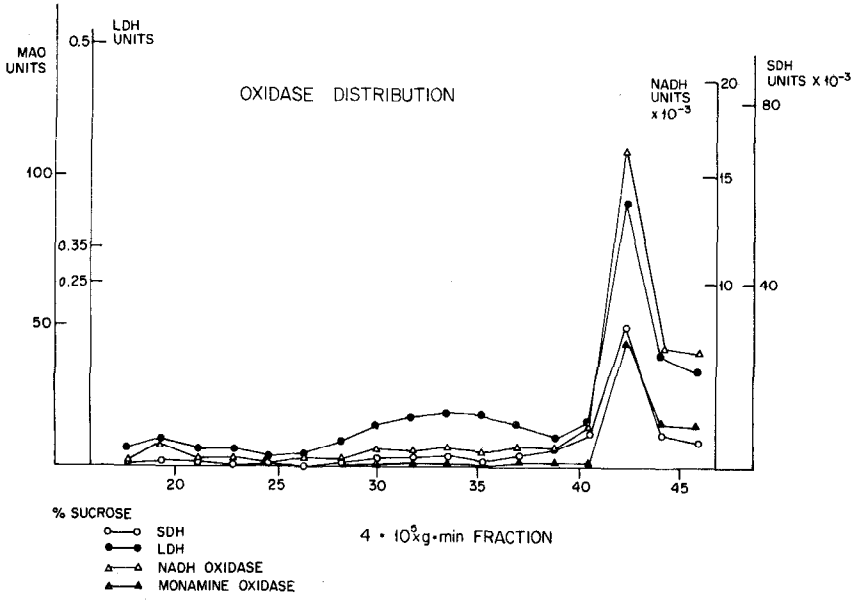

Fig. 5. Distribution of monamine oxidase (MAO), NADH oxidase, lactate dehydrogenase (LDH) and succinate dehydrogenase (SDH) in the gradient from the $4 \cdot 10^5 \times g \cdot$min precipitate.

Enzyme distribution

Oxidative enzymes. Succinic dehydrogenase, located on the inner membrane, and monoamine oxidase on the outer served as insoluble mitochondrial markers based on work with other tissues. On the gradient, the distribution of both these enzymes was unimodal, peaking in terms of total activity at 40.5 % (w/w) sucrose for the $1 \cdot 10^5 \times g \cdot$min fraction. The highest specific acitvity for succinate dehydrogenase was in the $1 \cdot 10^5 \times g \cdot$min band. Monamine oxidase has a higher specific activity in the $6 \cdot 10^6 \times g \cdot$min high density band (Figs 4–6).

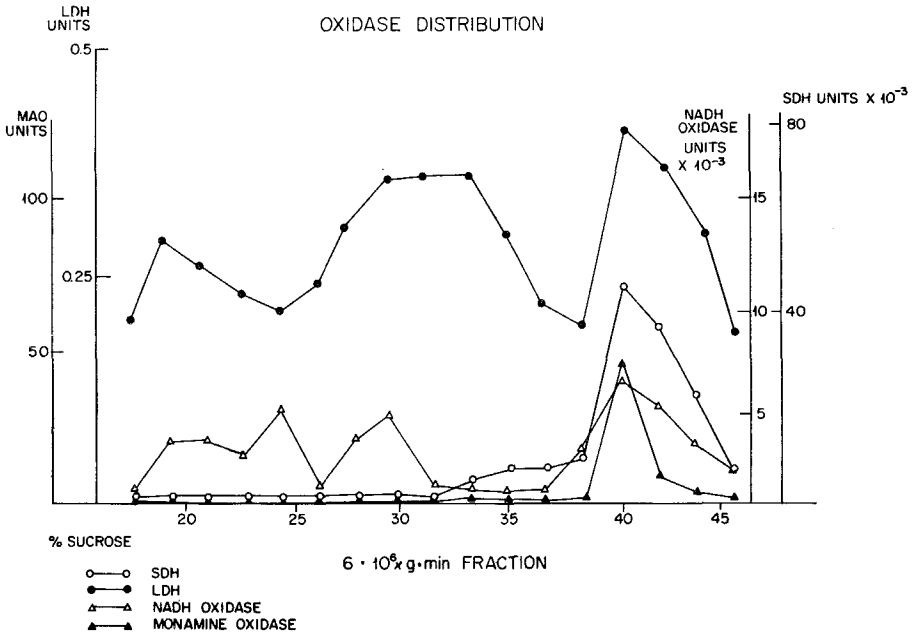

Fig. 6. Distribution of monamine oxidase (MAO), NADH oxidase, lactate dehydrogenase (LDH) and succinate dehydrogenase (SDH) in the gradient from the $6 \cdot 10^6 \times g \cdot$min precipitate.

Lactate dehydrogenase behaved largely like a soluble enzyme since most of the activity remained in the supernatant of the $6 \cdot 10^6 \times g \cdot$min fraction. However, some of the enzyme remained associated with the particulate fractions. Thus, in the gradient fractionated $1 \cdot 10^5 \times g \cdot$min material, part of the enzyme did not enter the gradient and part remained associated with the other enzyme markers at about 40.5 % sucrose. In the $4 \cdot 10^5 \times g \cdot$min and $6 \cdot 10^6 \times g \cdot$min fractions lactate dehydrogenase appeared to be mitochondrially bound, except for some activity peaking at about 32 % sucrose in the $6 \cdot 10^6 \times g \cdot$min fraction (Figs 4–6). Lactate dehydrogenase distribution in terms of specific activity had highest activity in the very light component of the $1 \cdot 10^5 \times g \cdot$min fraction, and in the soluble fraction of the homogenate.

NADH oxidase activity was largely associated with the > 40 % density material in all 3 fractions, but in addition a minor portion of the oxidase activity was associated with some lighter material especially in the $6 \cdot 10^6 \times g \cdot$min material (Figs 4–6). NADH oxidase specific activity was highest in the 27 % region of the $1 \cdot 10^5 \times g \cdot$min fraction.

Phosphatases. Acid phosphatase showed a complex distribution throughout the fractions. There was only a trace amount in the $1 \cdot 10^5 \times g \cdot$min fraction. However, a considerable amount is found in the $4 \cdot 10^5 \times g \cdot$min fraction banding on the gradient at the same density as the mitochondrial enzymes. Presumably this is due to admixture of the "light" mitochondria with lysosomes. In the $6 \cdot 10^6 \times g \cdot$min fraction acid phosphatase showed a bimodal distribution, peaking at 30 and 40.5 %. The highest specific activity was associated with the $6 \cdot 10^6 \times g \cdot$min fraction banding at 30 % sucrose (Figs 7–9) on the gradient.

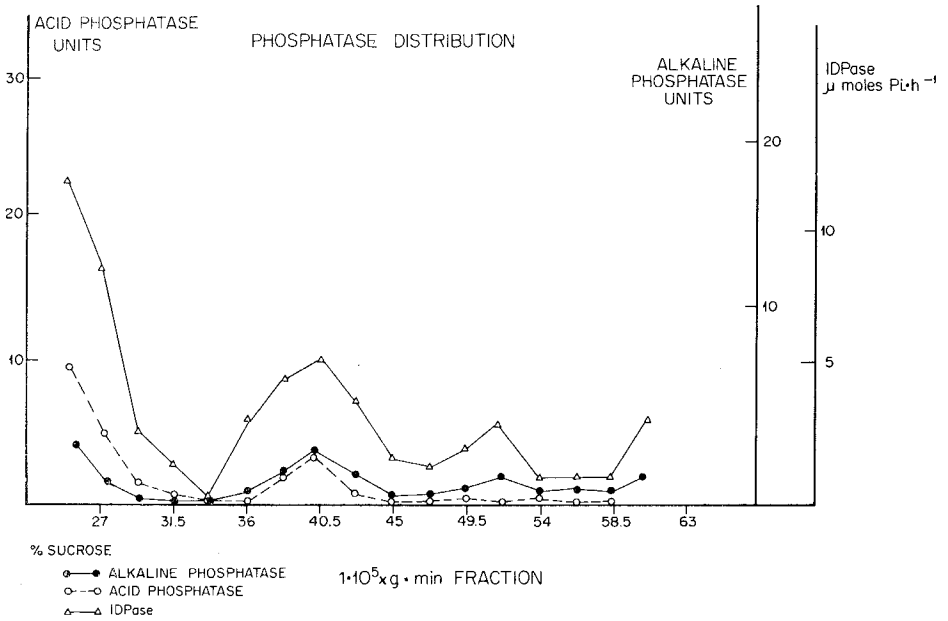

Fig. 7. Distribution of acid and alkaline phosphatase and inosine diphosphatase in the gradient from the $1 \cdot 10^5 \times g \cdot$min precipitate.

Alkaline phosphatase had only slight activity in the $1 \cdot 10^5$ and $4 \cdot 10^5 \times g \cdot$min fraction. In the $6 \cdot 10^6 \times g \cdot$min fraction peak activity occurred at a sucrose density slightly less than that for acid phosphatase, at about 28 % sucrose. Peak specific activity was similarly located (Figs 7–9).

Nucleoside mono- and di-phosphatases. Very little adenosine monophosphatase activity could be detected in any of the fractions examined. However, it is present in the $1000 \times g$ fraction, with this particular homogenization technique. Inosine diphosphatase was, however, present in all the fractions. In the $1 \cdot 10^5 \times g \cdot$min fraction the enzyme was associated with the 40.5 % band, and in the $4 \cdot 10^5 \times g \cdot$min fraction again mainly with the high density band. In terms of specific activity, however, the IDPase showed a peak at about 30 % in both the $4 \cdot 10^5 \times g \cdot$min and $6 \cdot 10^6 \times g \cdot$min fractions, with slightly higher activity in the latter (Figs 7–9).

Adenosine triphosphatases. As emphasized in the introduction, the precise localization of ATPase that is HCO_3^- stimulated is of prime importance in developing a hypothesis of the mechanism of acid secretion. Three ATPases were, therefore,

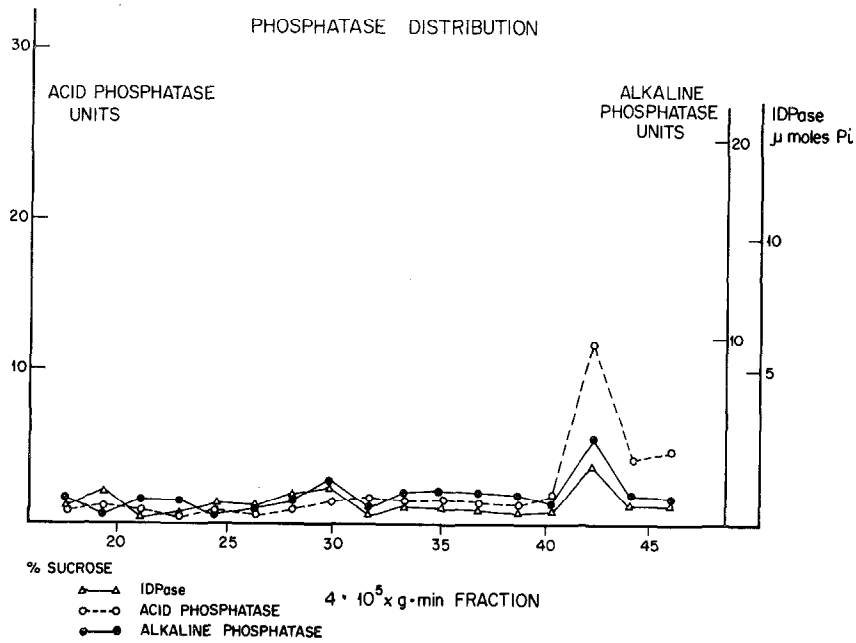

Fig. 8. Distribution of acid and alkaline phosphatase and inosine diphosphatase in the gradient from the $4 \cdot 10^5 \times g \cdot \text{min}$ precipitate.

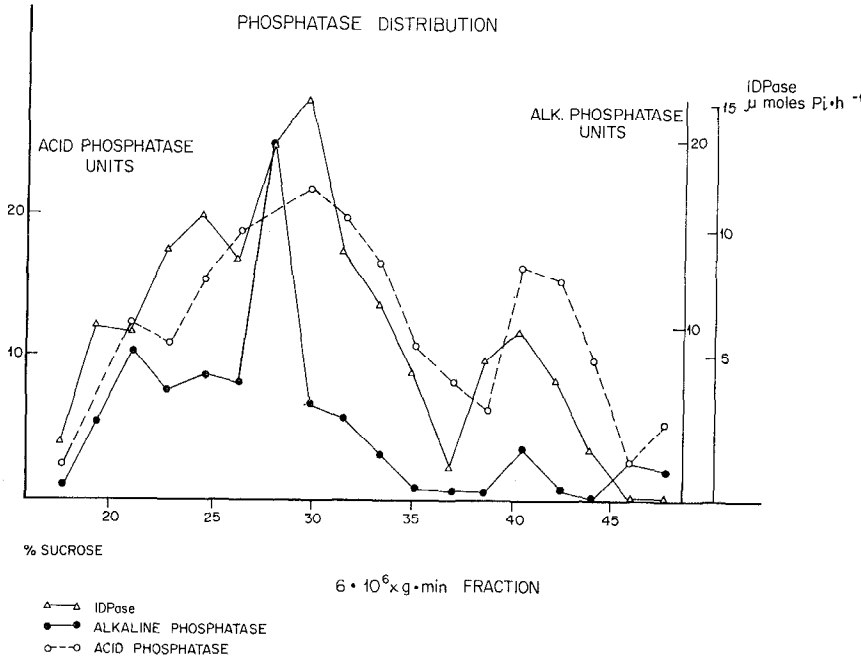

Fig. 9. Distribution of acid and alkaline phosphatase and inosine diphosphatase in the gradient from the $6 \cdot 10^6 \times g \cdot \text{min}$ precipitate.

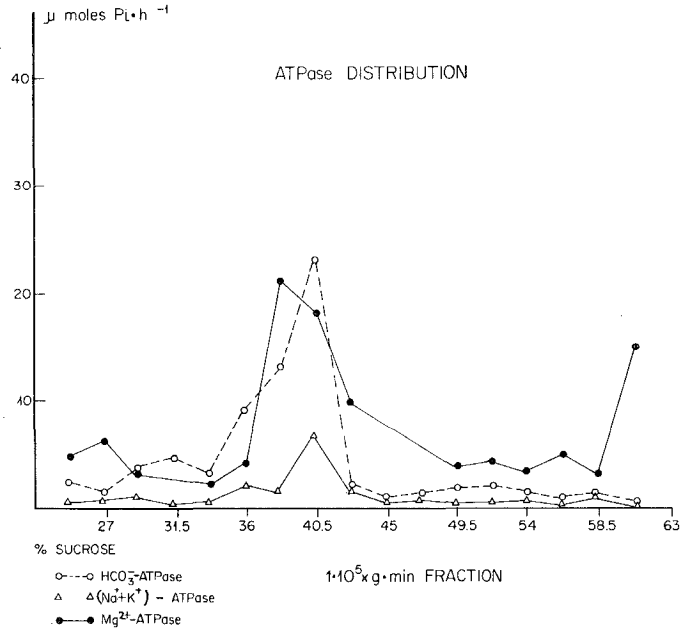

Fig. 10. Distribution of the HCO_3^--, $(Na^+ + K^+)$- and Mg^{2+}-ATPase in the gradient from the $1 \cdot 10^5 \times g \cdot$min precipitate.

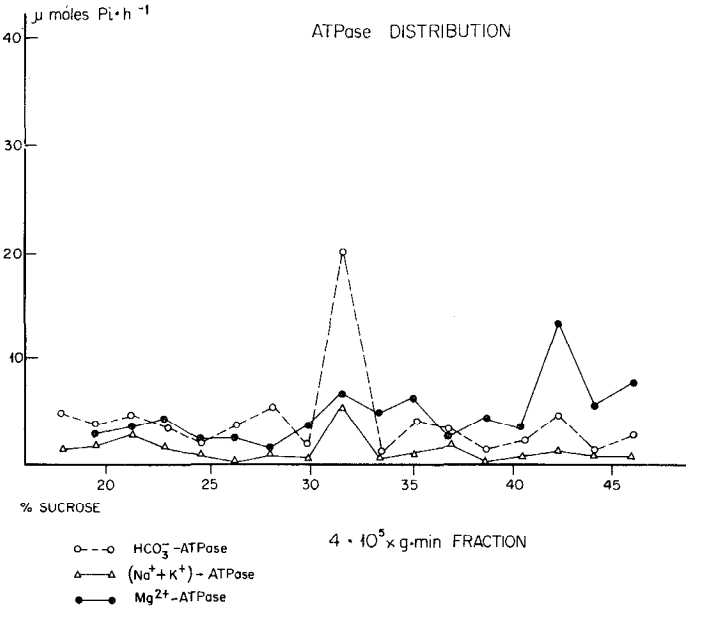

Fig. 11. Distribution of the HCO_3^--, $(Na^+ + K^+)$- and Mg^{2+}-ATPase in the gradient from the $4 \cdot 10^5 \times g \cdot$min precipitate.

studied: Mg^{2+}-dependent, (Mg^{2+} + $NaHCO_3$), and (Mg^{2+} + Na^+ + K^+)-ATPase. The (Na^+ + K^+)- and HCO_3^--ATPase activities were obtained by subtracting the Mg^{2+}-ATPase activity.

In the case of the $5 \cdot 10^5 \times g \cdot$min fraction there were 2 peaks of Mg^{2+}-ATPase, associated with the 31 % and the 42 % regions. However, the HCO_3^--ATPase showed essentially one major peak, at 31 % sucrose associated with a peak of the (Na^+ + K^+)-ATPase activity. The major HCO_3^--ATPase peak in this fraction, therefore, was not associated with any known mitochondrial markers (Fig. 11). In the $6 \cdot 10^6 \times g \cdot$min fraction, there were again 2 Mg^{2+}-ATPase peaks, at 27 and 40.5 % sucrose. HCO_3^--ATPase also showed a bimodal distribution corresponding to these 2 peaks, whereas the (Na^+ + K^+)-ATPase showed one low density peak. From these data, considerable (Na^+ + K^+)-ATPase is present in dog gastric mucosa. Thus in this fraction there was clearly a HCO_3^--sensitive ATPase which was non-mitochondrial, and a component which could be mitochondrial since it was associated with the mitochondrial markers, and not the (Na^+ + K^+)-ATPase membrane marker (Fig. 12).

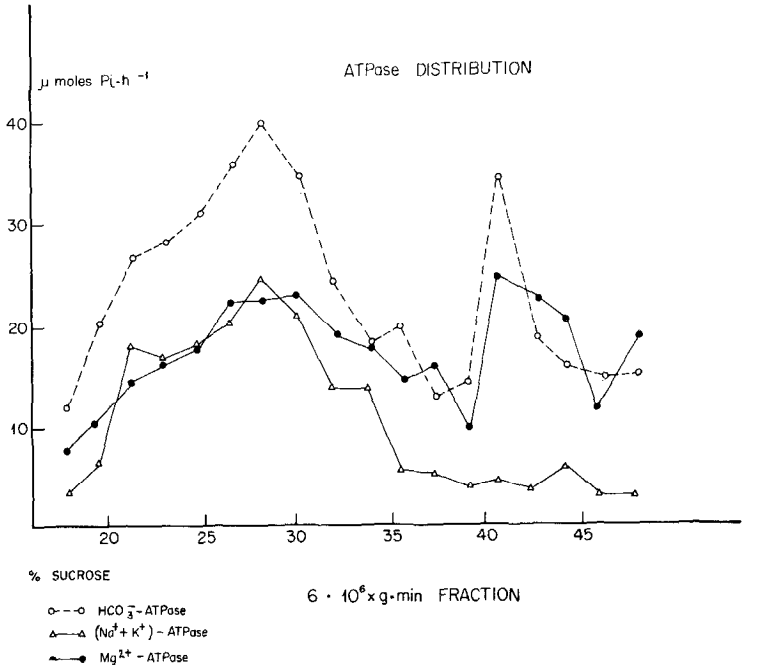

Fig. 12. Distribution of the HCO_3^--, (Na^+ + K^+)- and Mg^{2+}-ATPase in the gradient from the $6 \cdot 10^6 \times g \cdot$min precipitate.

The specific activity of the HCO_3^--ATPase was highest in the $4 \cdot 10^5 \times g \cdot$min 31 % band, followed by the 27 % from the $6 \cdot 10^6 \times g \cdot$min fraction. Table I shows the distribution ratios of all the enzymes from the various precipitates. This ratio is calculated as C/C_0 where C is activity in peak, C_0 is theoretical activity if enzyme were uniformly distributed. The values shown are for the HCO_3^--ATPase peak position and for the succinate dehydrogenase and monamine oxidase peak position. A ratio of > 1 shows concentration of enzyme activity. This table thus summarizes our findings.

TABLE I

ACTIVITIES OF ENZYMES IN GRADIENT FRACTIONS

The peak ratio is expressed as C/C_0, where C is activity in peak tube, *i.e.* 40.5% region for the $1 \cdot 10^5 \times g \cdot$min band, and 29.5 (a) and 40.5% (b) bands for the $4 \cdot 10^5 \times g \cdot$min and $6 \cdot 10^6 \times g \cdot$min band, and C_0 is theoretical activity if the activity were uniformly distributed through the gradient.

Enzyme	*Peak ratio*				
	$1 \cdot 10^5 \times g \cdot min$	$4 \cdot 10^5 \times g \cdot min$		$6 \cdot 10^6 \times g \cdot min$	
		(a)	(b)	(a)	(b)
HCO_3^--ATPase	6	12.3	<0.1	2	1.4
$(Na^+ + K^+)$-ATPase	3	3.1	<0.1	3.5	0.1
Mg^{2+}-ATPase	5	1.4	2.1	1.3	1.4
IDPase	1.2	0.2	3.6	2.5	1
Alkaline phosphatase	3	0.5	7	5	0.5
Acid phosphatase	2.3	<0.1	5	2	1.3
Succinate dehydrogenase	7.5	<0.1	10	<0.1	5
Monamine oxidase	9	<0.1	12	<0.1	12
Lactate dehydrogenase	2.5	0.2	5	2.4	2.9
NADH oxidase	3.8	<0.1	7.5	2.1	2.7

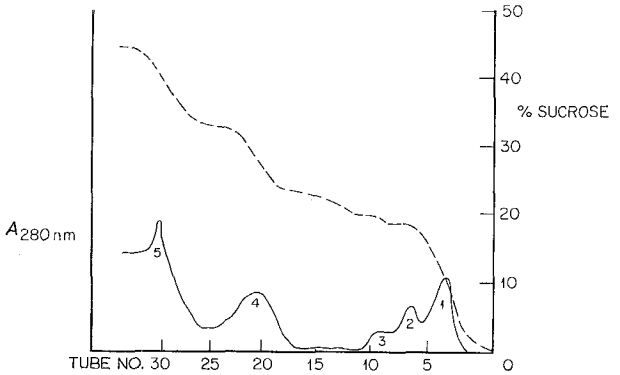

Fig. 13. Zonal runs of the $6 \cdot 10^6 \times g \cdot$min precipitate on a discontinuous sucrose gradient of 20, 24, 34 and 47% sucrose on a Beckman B14 rotor at 0 °C for 5 h at 30000 rev./min.

Zonal centrifugation. Based on the above data a rate centrifugation was carried out, on a discontinuous gradient of 20, 24, 34 and 47% sucrose for 4 h at 30000 rev./min in a Beckman B14 rotor. Fig. 13 shows the protein distribution and the measured sucrose concentration and Table II the activity of HCO_3^--ATPase in each 20-ml fraction. It can be seen that there is sharp separation of activity of the HCO_3^--ATPase, as well as considerable heterogeneity of the lighter particles.

Effect of solubilization. Triton X-100 solubilization of the two ATPase peaks from the density gradient fractionated $6 \cdot 10^6 \times g \cdot$min material results in a large increase in the HCO_3^- activation of enzyme for both peaks. Both enzymes are also stimulated by arsenate and inhibited by CNO^-. Thus although the two enzymes are readily distinguished by their density in the particulate form, once solubilized they display remarkably similar characteristics (Table III), except that the enzyme from the heavier fraction appears to be more sensitive to CNO^-.

TABLE II

ACTIVITY OF BANDS FROM ZONAL ROTOR

These activities were determined on fractions from zonal rotor bands 1–5 from Fig. 13.

Band	*HCO_3^--ATPase activity* ($\mu moles\ P_i \cdot mg^{-1}$)
1	0.251
2	3.73
3	4.50
4	26.55
5	11.91

TABLE III

ACTIVITY OF SOLUBILIZED ATPase IN THE $6 \cdot 10^6 \times g \cdot$min FRACTION

	30.5% peak ($\mu moles\ P_i \cdot mg^{-1} \cdot h^{-1}$)	*40.5% peak* ($\mu moles\ P_i \cdot mg^{-1} \cdot h^{-1}$)
Mg^{2+}	17.1	14.1
$Mg^{2+} + HCO_3^-$	58.3	63.6
$Mg^{2+} + AsO_2^-$	71.4	48
$Mg^{2+} + CNO^-$	8.4	0.8

DISCUSSION

Recently it has been shown[15] that mitochondrial ATPase in some preparations of rat liver mitochondria can be stimulated by a variety of anions such as chromate, sulfate, arsenate, *etc.*, as well as being inhibited by thiocyanate SCN^- inhibition had previously been shown in intact mitochondria. Evidently, therefore, the demonstration that a variety of oxyanions can stimulate an ATPase present in *Necturus* oxyntic cells[8], mammalian gastric mucosa[9] and pancreas (B. Simon, R. Kinne and G. Sachs, to be published), from a vesicular fraction that did not have morphology or density suggestive of mitochondria was of interest, but required further documentation.

From the results presented here, no mitochondrial enzyme marker was present in the low density HCO_3^--ATPase fraction. Only alkaline phosphatase seemed to have an approximately similar distribution, absent in the soluble form. Since the morphology of the active fraction corresponded to that expected from the vesicles of oxyntic cells, we concluded that an anion stimulated, SCN^- or CNO^- inhibited ATPase is indeed a constituent of the secretory membrane of the gastric cell. 5′-Nucleotidase was absent from this fraction, but is present in the plasma membrane banding at 5% ficoll (J. G. Spenney and G. Sachs, unpublished), showing separation between the two types of membrane is possible.

The occurrence of similar ATPases in the membrane of the gastric cell and mitochondria suggests there may be a functional similarity between proton transport at the intracellular canaliculi of the parietal cell and coupling of redox reaction to ATP formation in the mitochondria.

One such possibility is illustrated in Fig. 14a. Here the ATPase I scheme[16] of Mitchell is modified to allow for the reactivity of HCO_3^- and other anions. The result of this is transport of OH^- away from the luminal surface of the gastric oxyntic cell by the action of the ATPase located on the inner face of the membrane. Carbonic anhydrase intervenes to produce HCO_3^- which may be more readily transported. In redox theory, OH^- could originate by reduction of O_2 by electrons from the respiratory chain. Usually, this is written as flow of electrons to one side of the membrane, and protons out of the other side, the location of the redox carriers giving the vectorial characteristics to the system[16].

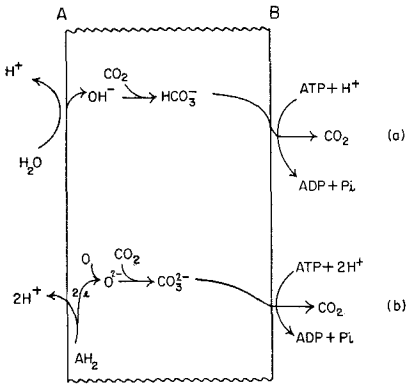

Fig. 14. Provisional models for a role of the HCO_3^--ATPase in acid secretion. (a) A modified ATPase I scheme of Mitchell[16] and (b) a combined redox and ATPase model.

Alternatively, the redox reaction can be written so that O^{2-} is produced at the same side as the proton, and an ATPase translocator removes the O^{2-} following reaction with CO_2 to form CO_3^{2-} as in the ATPase I scheme (Fig. 14b). Once again, the scheme is modified to allow for the reactivity of the CO_3^{2-} as in the ATPase I scheme (Fig. 14b). Once again, the scheme is modified to allow for the reactivity of CO_3^{2-} in the reaction. The reactivity of O^{2-} is such, that in the presence of CO_2, for which there is unlikely to be a diffusion barrier, the half life of O^{2-} is likely to be very small. Hence it is quite likely that CO_3^{2-} is translocated rather than O^{2-} by any ATPase translocator existing either in mitochondria or gastric secretory membrane. Similar considerations apply to OH^- and HCO_3^-. These considerations may account for the rather general oxyanion stimulation found for these enzymes[9,15].

The combination of an ATP and redox theory may account for the observation that SCN^- does not inhibit O_2 consumption by more than 20% in the secreting mucosa[17], since in this model SCN^- would inhibit removal of the reduction product of the reaction (which could then recombine with H^+), but not the flow of electrons to O_2. Hence O_2 consumption would be only partially inhibited, depending on the HCO_3^-/ATP ratio.

Therefore, the ATPase described here, and in previous publications, may be the primary enzyme in proton transport either solely or coupled with a redox reaction, both in mitochondria and gastric mucosa.

ACKNOWLEDGEMENT

This work was supported by N.I.H. Grant AM08451 and N.S.F. Grants GB8351 and GB25364,

One of the authors (A.S.) is a Trainee of N.I.H. Gastroenterology Training Grant TIAM05286.

REFERENCES

1 D. K. Kasbekar and R. P. Durbin, *Biochim. Biophys. Acta*, 105 (1965) 472.
2 G. Sachs, W. E. Mitch and B. I. Hirschowitz, *Proc. Soc. Exp. Biol. Med.*, 119 (1965) 1023.
3 J. G. Forte, G. M. Forte and R. F. Bils, *Exp. Cell Res.*, 42 (1966) 662.
4 G. M. Forte, L. Limlomwongse and J. G. Forte, *J. Cell Sci.*, 4 (1969) 709.
5 E. Racker, *Fed. Proc.*, 21 (1962) 54A.
6 G. Sachs, R. H. Collier, R. L. Shoemaker, A. Pacifico and B. I. Hirschowitz, *Biochim. Biophys. Acta*, 173 (1969) 509.
7 G. Sachs, R. H. Collier and B. I. Hirschowitz, *Proc. Soc. Exp. Biol. Med.*, 133 (1970) 456.
8 V. D. Wiebelhaus, C. P. Sung, H. F. Helander, G. Shah, A. L. Blum and G. Sachs, *Biochim. Biophys. Acta*, 241 (1971) 49.
9 A. L. Blum, G. Shah, T. St. Pierre, H. F. Helander, C. P. Sung, V. D. Wiebelhaus and G. Sachs, *Biochim. Biophys. Acta*, 249 (1971) 101.
10 T. E. King and R. L. Howard, in *Methods in Enzymology*, Vol. 10, Academic Press, New York, 1967, p. 275.
11 T. E. King, in *Methods in Enzymology*, Vol. 10, Academic Press, New York, 1967, p. 322.
12 A. Yoda and L. E. Hokin, *Biochem. Biophys. Res. Commun.*, 40 (1970) 880.
13 C. W. Tabor, H. Tabor and S. M. Rosenthal, *J. Biol. Chem.*, 208 (1954) 645.
14 W. J. Reeves and G. M. Fimognari, in *Methods in Enzymology*, Vol. 9, Academic Press, New York, 1966, p. 288.
15 P. Mitchell and J. Moyle, *Bioenergetics*, 2 (1971) 1.
16 P. Mitchell, in E. Bittar, *Membranes and Ion Transport*, Vol. I, Wiley, 1970.
17 F. G. Moody, *Am. J. Physiol.*, 220 (1971) 467.